Turkish Journal of Electrical Engineering & Computer Sciences

http://journals.tubitak.gov.tr/elektrik/

Research Article

Turk J Elec Eng & Comp Sci
(2020) 28: 799 – 820

doi:10.3906/elk-1901-182

Robust optimal operation of smart distribution grids with renewable based generators

Omid ZARE SEHSALAR[1], **Sadjad GALVANI**[1,2,*], **Murtaza FARSADI**[1,2]
[1]Department of Electrical Engineering, Faculty of Engineering, Urmia Branch, Islamic Azad University, Urmia, Iran
[2]Department of Power Engineering, Faculty of Electrical and Computer Engineering, Urmia University, Urmia, Iran

Received: 26.01.2019 • **Accepted/Published Online:** 26.12.2019 • **Final Version:** 28.03.2020

Abstract: Modern distribution systems are equipped with various distributed energy resources (DERs) because of the importance of local generation. These distribution systems encounter more and more uncertainties because of the ever-increasing use of renewable energies. Other sources of uncertainty, such as load variation and system components' failure, will intensify the unpredictable nature of modern distribution systems. Integrating energy storage systems into distribution grids can play a role as a flexible bidirectional source to accommodate issues from constantly varying loads and renewable resources. The overall functionality of these modern distribution systems is enhanced using communication and computational abilities in smart grid frameworks. Robust operation of these systems is effectively taken into consideration to manage the uncertainty, which offers an explicit way to control the desired conservativeness. This paper presents an optimal operating program for smart grids equipped with wind generators, controllable distributed generators, energy storage systems, and reactive power compensators. In order to make the studies more practical, uncertainty about wind generators and grid loads is taken into account. Furthermore, the presented operating program is robust in various conditions, i.e. there is no need to change the operating program in a wide range of probable states. The point estimation method and fuzzy clustering method are used for probabilistic assessment of the distribution system in the presence of uncertainties. The IEEE 37-node standard test system, which is a highly unbalanced system, is selected for the case study and the results are discussed comprehensively.

Key words: Fuzzy clustering method, particle swarm optimization, point estimation method, probabilistic assessment, robust operating, smart distribution grid

1. Introduction

1.1. Motivation

Conventional power grids have a hierarchical structure, transferring electricity through the upstream transmission networks to the loads in distribution networks. The conventional structure of power grids has remained unchanged for many years. Some of the most important problems in these grids are inefficiency of the power grid in managing the maximum demand, control of renewable energy sources, exchanging reliable information, withstanding some probable events, and so on. In smart distribution grids, many of these problems can be efficiently managed by reliable control of power generation, storage, and consumption using communication and computational abilities.

Distributed energy resources (DERs) have salient technical and economical benefits in distribution systems such as increased resiliency and reduced losses. They are divided into two general groups: control-

*Correspondence: s.galvani@urmia.ac.ir

lable/dispatchable and noncontrollable/nondispatchable. Dispatchable ones such as combined heat and power (CHP) generators can change their output fairly quickly in order to meet electricity demands. However, nondispatchable ones are completely unpredictable and intermittent, and they are not continuously available due to factors that cannot be controlled, such as weather conditions. Their unpredictable nature brings out many challenges in operating programs. These challenges are made more complicated by other uncertainty sources such as load variations and system components' failures. Energy storage systems (ESSs) have become a critical issue in balancing the generations and the loads since they provide the ability to reach maximum efficiency from renewable resources with a more uniform output profile. On the other hand, robust operating programs can also effectively deal with uncertainties and satisfy a wide range of probable operating conditions.

Based on the mentioned points, optimal operation is of great importance in smart distribution grids as it includes probabilistic constraints and is robust in different operating conditions (so that with adjustment of control variables once, more hours of grid conditions are covered), and it reduces the risk of decision-making for grid operators. In this relation, probabilistic evaluation methods will be more efficient if they can produce accurate results with little computational complexity [1].

1.2. Literature review

Many studies have addressed the operation of smart distribution systems. In some references, energy management in microgrids, including ESSs, has been studied and the uncertainty associated with renewable-based generators and loads has been considered. However, none of these studies considered the grid model and its associated operating constraints.

In this regard, [2] focused on reducing the final cost of energy supplies, while [3] paid attention to various components of operational cost, such as the cost of thermal generation, the cost of purchased power from the upstream grid, and the cost of energy storage resources. The work in [4] investigated reliable energy supplies with the lowest cost. In [5], the cost of pollution and maintenance costs associated with power generation were considered along with other cost components. In [6], long-term costs including investment, maintenance, fuel, and emission costs were also considered. The authors of [7] referred to the cost of distributed generation power plants and the purchase of power from the upstream grid. In [8], the economic component was taken into account with respect to the optimal cost of energy storage, while [9] examined the reduction of the total cost of energy supplies with respect to the price of energy usage time. The work in [10] evaluated the reduction of the energy imbalance caused by the online differences of energy between conventional supply, real demand, and corresponding costs. Reducing the expected cost during the grid planning horizon was discussed in [11]. In [12], creating a trade-off between reducing the cost of power generation and the amount of charging and discharging the energy storage was considered. The authors of [13] focused on increasing the profit and reducing the total cost of thermal power plant operation.

Furthermore, in many other references, energy management in distribution systems including ESSs was taken into account and the uncertainty caused by renewable generators and load was considered. None of these studies paid attention to the robustness of the operating program.

In this regard, [14] considered the reduction of total costs and losses, while [15] reduced operational costs and improved the performance quality of distribution systems. Reducing losses by maintaining all grid operating limits was addressed in [16], while [17] studied the improvement of voltage and current controllability. In [18], loss reduction and more profitability were considered with energy arbitrage. In [19], increasing

reliability was considered. In [20], similar to [19], increasing profitability was considered. Controllable power plant cost, blackout, and start-up costs were taken into consideration in [21]. The reliability assessment of distribution systems having both controllable and uncontrollable resources was investigated in [22]. In [23], more participation of energy storage systems in the energy management of distribution grids was considered. The work in [24], considering reactive power compensators and energy storages, reduced the active power losses in distribution grids. In [25], reducing the cost of exchanging power between energy storage systems with a robust approach was considered. The formulation of a short-term load shedding program was reviewed in [26]. In [27], the reduction of the unbalancing amount of main feeder flow, losses, and greenhouse gas emissions was investigated. Although grid models, losses, and related operational limitations were considered in these studies, the robustness of the operating point has not been contemplated, as previously said.

On the other hand, obtaining a fast operating program is very important especially in online applications. Calculation burden reduction will be more necessary in probabilistic studies. Recently, clustering methods have been considered in power system probabilistic studies [28–32]. The task of organizing a collection of objects in such a way that objects within the same group are more similar to one another than to those in other groups is called clustering. In probabilistic studies of power systems, researchers have employed different kinds of clustering methods. There are five different clustering categories: partitional clustering such as K-means, agglomerative clustering such as hierarchical, fuzzy clustering such as fuzzy C-means, neural network-based clustering such as self-organizing maps, and various types of bioinspired clustering methods [33]. Clustering methods require a very low calculation burden, they have acceptable levels of accuracy, they can be applied to every type of uncertain variables, and consequently they are suitable for online and practical applications.

1.3. Paper contribution

As can be seen from the review of related publications in recent years, introducing an operating program for smart grids in the presence of uncertainties is very important.

As its main contribution, this paper provides a robust optimal operating program in the presence of nondispatchable renewable-based distributed generators, ESSs, dispatchable power generation sources such as CHP generators, and reactive power compensators while satisfying all operational constraints. The proposed operating program does not need to change in various time intervals in which the condition of the distribution system is continuously changing. In addition, two efficient methods are used for probabilistic assessment of the distribution system in this work: the point estimation method (PEM) and fuzzy clustering method (FCM). PEM and FCM have been previously used for probabilistic assessment of power systems, but their applications in robust operation of distribution systems are being evaluated for the first time in this paper. These methods are comprehensively compared to each other regarding calculation time aspects. None of the references mentioned above considered these related issues all together.

1.4. Paper structure

The rest of the paper is organized as follows. In Section 2, uncertainties are modeled mathematically. In Section 3, the probabilistic assessment method used in this paper is presented. The problem formulation is given in Section 4. Then the optimization method is discussed in Section 5. Section 6 presents the case study and the obtained results. Finally, the conclusion is given in Section 7.

2. Uncertainty modeling

2.1. Loads

Load uncertainty is often modeled by a normal probability distribution. In this study, active load demand is considered as a normally distributed random variable, and reactive load demand is obtained by considering a constant power factor. The probability density function (PDF) of the ith bus's active load demand is formulated according to 1 [34]:

$$\mathrm{PDF}\left(P_i^{\mathrm{Load}}\right) = \frac{1}{\sqrt{2\pi}\sigma\left[P_i^{\mathrm{Load}}\right]} e^{\frac{\left(P_i^{\mathrm{Load}} - \mathrm{E}\left[P_i^{\mathrm{Load}}\right]\right)^2}{2\sigma\left[P_i^{\mathrm{Load}}\right]^2}}, \tag{1}$$

where P_i^{Load} is the active load demand at the ith node, and $\sigma[]$ and $\mathrm{E}[]$ denote the standard deviation and mean value operators, respectively.

2.2. Wind generation

The Weibull distribution is conventionally used for modeling of wind speed PDF. However, wind generator output is commonly expressed by this PDF as in 2 [34]:

$$\mathrm{PDF}\left(P_i^{\mathrm{Wind}}\right) = \begin{cases} \frac{k}{\lambda}\left(\frac{P_i^{\mathrm{Wind}}}{\lambda}\right)^{(k-1)} \times e^{-\left(\frac{P_i^{\mathrm{Wind}}}{\lambda}\right)^k} & P_i^{\mathrm{Wind}} \geq 0 \\ 0 & \text{other,} \end{cases} \tag{2}$$

where P_i^{Wind} is the active power generation of the wind generator located at the ith node. λ and k are the scale parameter and the shape parameter of Weibull distribution, respectively.

3. Probabilistic evaluation of power systems

Power systems are encountered with high levels of uncertainties due to the unpredictable output of renewable generations, loads variation, probable failure of system components, etc. Several methods have been used for probabilistic assessment of power systems in the presence of uncertainties. These methods are generally classified into three categories of Monte Carlo simulations (MCSs), analytical methods, and approximation methods. The MCS method has been widely used to assess uncertainties in power systems. The basic weakness of the MCS method is requiring a large number of simulations in order to achieve convergence. Analytical methods are very efficient in terms of computational burden but these methods also require some mathematical simplifications such as the linearization of the problems. Approximation methods provide an approximate description from the probabilistic properties of output random variables. These methods require much lower computational complexity and do not require full information about the probability distribution of input random variables compared to the MCS method.

Data clustering and PEMs are two types of approximation methods that have been widely used in probabilistic assessment of power systems. PEMs are very simple and do not require the computation of derivatives [35, 36]. However, the accuracy of these methods is low in estimating high-order moments of probability distributions. Also, their calculation burden rapidly increases for large systems with many input random variables. Data clustering methods are very easy to implement and they are very efficient in large systems with many input numbers [37].

3.1. Point estimation method

The purpose of all PEMs is to calculate the statistical moments of the output random variable Z, which is a function of M input random variables P_m as in (3):

$$Z = F\left(p_1, p_2, ..., p_m, ..., p_M\right). \tag{3}$$

The point estimation methods concentrate the statistical information of the input random variables (which is available via several central moments) on K points, which are called the concentrations.

The Kth concentration of the random variable P_m $(p_{m,k}, w_{m,k})$ is defined as a pair of location $p_{m,k}$ and weight $w_{m,k}$. The location of $p_{m,k}$ is the Kth amount of random variable P_m and weight $w_{m,k}$ is the coefficient that shows the relative importance of this location.

Using the Hong method, the F function is evaluated K times for each input random variable P_m in the K points. These points are formed from the kth place of the P_m $(p_{m,k})$ and the average value of other $M-1$ random input variables $\left(\mathrm{E}\left[p_1\right], \mathrm{E}\left[p_2\right], ..., p_{m,k}, ..., \mathrm{E}\left[p_M\right]\right)$.

The value of K for evaluating each variable depends on the type of used method. Thus, the total value of F function evaluation is $K \times M$. The $2 \times M$ method is explained as follows. The locations $p_{m,1}$ and $p_{m,2}$ associated with the mth random variable are determined from input statistical information by (4) and (5):

$$p_{m,1} = \mathrm{E}\left[p_m\right] + \xi_{m,1} \times \mathrm{SD}\left[p_m\right], \tag{4}$$

$$p_{m,2} = \mathrm{E}\left[p_m\right] - \xi_{m,2} \times \mathrm{SD}\left[p_m\right]. \tag{5}$$

In these equations, $\xi_{m,1}$ and $\xi_{m,2}$ are standard locations, $\mathrm{E}\left[\mathrm{p_m}\right]$ is the average value of p_m, and $\mathrm{SD}\left[\mathrm{p_m}\right]$ is the standard deviation amount of the random variable p_m.

The standard locations are obtained from (6) and (7):

$$\xi_{m,1} = \frac{\lambda_{m,3}}{2} + \sqrt{M + \left(\frac{\lambda_{m,3}}{2}\right)^2}, \tag{6}$$

$$\xi_{m,2} = \frac{\lambda_{m,3}}{2} - \sqrt{M + \left(\frac{\lambda_{m,3}}{2}\right)^2}, \tag{7}$$

where $\lambda_{m,3}$ is the third central moment of p_m.

Also, the weight coefficients are obtained from (8) and (9):

$$w_{m,1} = -\frac{1}{M} \times \frac{\xi_{m,2}}{\xi_{m,1} - \xi_{m,2}}, \tag{8}$$

$$w_{m,2} = -\frac{1}{M} \times \frac{\xi_{m,1}}{\xi_{m,1} - \xi_{m,2}}. \tag{9}$$

After obtaining all locations and their weights the function F is evaluated in the $\left(\mathrm{E}\left[p_1\right], \mathrm{E}\left[p_2\right], ..., p_{m,k}, ..., \mathrm{E}\left[p_M\right]\right)$ point and $Z(m,k) = F\left(\mathrm{E}\left[p_1\right], \mathrm{E}\left[p_2\right], ..., p_{m,k}, ..., \mathrm{E}\left[p_M\right]\right)$ is obtained. Finally, using the weight coefficients, the

jth moment of the output variable Z can be obtained according to (10), in which Z is the vector of the output variables [36]:

$$\mathrm{E}\left[\mathrm{Z}^{\mathrm{j}}\right] = \sum_{\mathrm{m}=1}^{\mathrm{M}} \sum_{\mathrm{k}=1}^{2} \mathrm{w}_{\mathrm{m,k}} \times \mathrm{Z}_{\mathrm{m,k}}{}^{\mathrm{j}}. \tag{10}$$

Figure 1 shows the flowchart of the two-point estimation method.

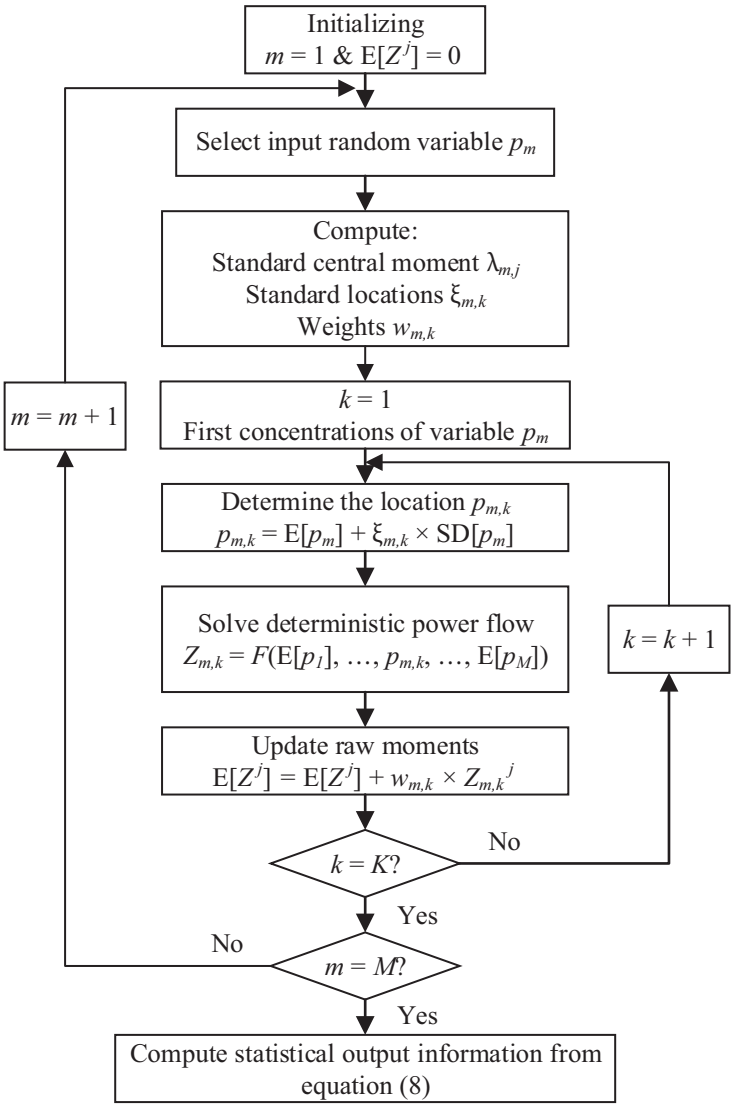

Figure 1. Flowchart of probabilistic assessment using PEM.

3.2. Fuzzy clustering method

The clustering technique refers to dividing data into subclasses called clusters based on their similarity. In each cluster, data appear to be more similar to one another and less similar to other data. Euclidean distance is

generally used for stating the similarity. Objects that are closer to one another are considered as a cluster, and an agent is designated to each cluster. Instead of analyzing all data, only agents are assessed. Fuzzy C-means (FCM) is one of the data clustering methods introduced by Dunn in 1973 [38]. This algorithm presents fuzzy behavior, and data are placed in clusters based on their membership coefficients. Membership coefficients are numbers between 0 and 1 and represent the degree of membership between data and clusters' agents. In this method, one piece of data may belong to two or more clusters. The steps of this algorithm are summarized as follows [39]:

Suppose $\mathbf{P}$ to be an M-dimensional vector of input random variables as $\mathbf{P} = [\mathbf{p_1}, \mathbf{p_2}, ..., \mathbf{p_M}]^{\mathrm{T}}$. Each $\mathbf{p_i}$ has N observations and $\mathbf{P}$ is an $N \times M$ matrix where each row is stated as on observation or datum called $\mathbf{d}_n$, $n = 1, 2, ..., N$.

Step 1 K, the number of the clusters, is selected.

Step 2 An agent $\mathbf{a_k}$ is randomly selected for each cluster from the entire data space where $k = 1, 2, ..., K$.

Step 3 The matrix of membership coefficients $\mathbf{U}$ is calculated. The nth row and kth column element of this matrix is obtained according to (11):

$$u_{nk} = \frac{1}{\sum_{l=1}^{K} \left(\frac{|\mathbf{d_n} - \mathbf{a_k}|}{|\mathbf{d_n} - \mathbf{a_l}|} \right)^{\frac{2}{m-1}}}, \tag{11}$$

where u_{nk} is the degree of membership of $\mathbf{d_n}$ in $\mathbf{a_k}$. Also, $\mathbf{d_n}$ denotes the nth data; $\mathbf{a_k}$ and $\mathbf{a_l}$ indicate the kth and lth agents, respectively; and m denotes fuzzification constant and $1 < m < \infty$. Higher values of m lead to higher levels of fuzziness.

Step 4 Agents of categories are updated based on (12):

$$\mathbf{a_k} = \frac{\sum_{n=1}^{N} {u_{nk}}^m . \mathbf{d_n}}{\sum_{n=1}^{N} {u_{nk}}^m}. \tag{12}$$

Step 5 Steps 3 and 4 are repeated until the changes in the agents are limited to a prespecified threshold.

Step 6 A probability is assigned to each agent as in (13):

$$\mathrm{p}\left(\mathbf{a_k}\right) = \frac{\mathrm{N_{G_k}}}{\mathrm{N}}, \tag{13}$$

Where N_{G_k} is the number of data points belonging to the kth cluster and N is the total number of data.

Each cluster agent is applied to the power flow problem as an input, and its corresponding output is saved. The statistical moments of output variables Z are obtained according to (14):

$$\mathrm{E}\left[Z^i\right] = \sum_{k=1}^{K} \mathrm{p}\left(\mathbf{a_k}\right) \cdot F(\mathbf{a_k})^i, \tag{14}$$

where $F(\mathbf{a_k})$ indicates the output of the power flow problem by considering $\mathbf{a_k}$ as the input.

Figure 2 shows the flowchart of the fuzzy clustering method.

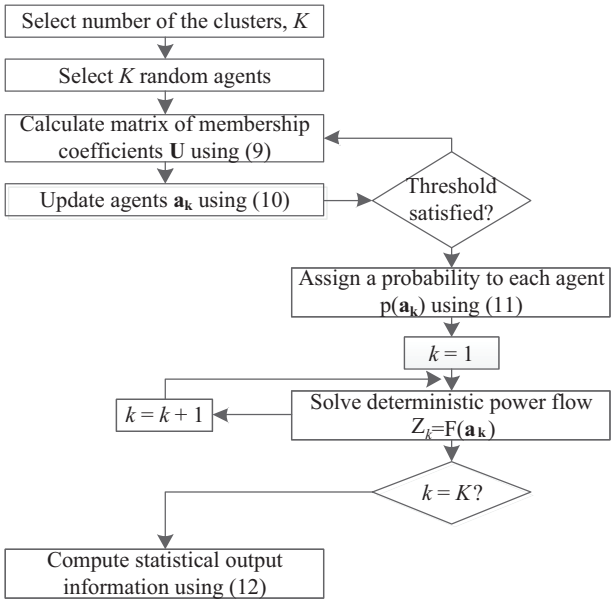

Figure 2. Flowchart of probabilistic assessment using FCM.

4. Problem formulation

4.1. Objective function

The objective function is defined according to (15). The objective function is the expected operating cost and it has two components: the first component is the expected cost of active power bought from the upstream transmission grid during the whole studying interval $(t = 1, 2, ..., T)$ and the second component is the expected cost of active power generation in all CHP units $(i = 1, 2, ..., N_{CHP})$ during the whole studying interval $(t = 1, 2, ..., T)$:

$$F(x) = \sum_{t=1}^{T} \left(w1_t \times \mathrm{E}\left[{P_t}^{\mathrm{Transmision}} \right] \right) + \sum_{t=1}^{T} \left(\sum_{i=1}^{N_{\mathrm{CHP}}} w2_{t,i} \times {P_{t,i}}^{\mathrm{CHP}} \right). \tag{15}$$

In this expression, T is the number of studied time periods and $\mathrm{E}\left[{P_t}^{\mathrm{Transmision}} \right]$ is the expected amount of active power taken from the upstream transmission grid at the tth time period. $w1_t$ is the active power conversion coefficient taken from the upstream transmission grid to the cost. N_{CHP} is the number of dispatchable (CHP) generators available in the grid. ${P_{t,i}}^{\mathrm{CHP}}$ is the active power of the ith CHP generator at the tth time period. $w2_{t,i}$ is the active power conversion coefficient of the ith CHP output to the cost at the tth time period.

In (15), it is assumed that renewable-based generators already exist in the grid. Hence, installation, start-up, repairing, and maintenance costs as well as other costs associated with these generators are not present in the objective function. It is also assumed that reactive power compensators already exist in the power grid and are installed in certain places, so the costs associated with their installation and start-up, repairing, and

maintenance are not present in the objective function. Also, assuming that energy storage systems already exist in the grid and have been installed in certain places, the costs associated with their installation and start-up, repair, and maintenance and other associated costs have not been included in the objective function.

4.2. Control variables

In (15), the control variables include the tap position of transformers in the distribution grid, the amount of active power produced by CHP stations, the reactive power amount of VAr compensators, and the amount of charge and discharge of energy storage systems during the study periods.

4.3. Constraints

Constraints related to this optimization problem include the constraints of nodal power balancing, the constraints on the control variables, and the constraints on the state variables. Power balancing constraints are according to (16) and (17), the constraints of the control variables are in accordance with (18) to (20), and the constraints of the power system state variables are in accordance with (21) to (25). However, in the probabilistic environment, the magnitude of state variables like the voltage of the nodes or the current flow in feeders is replaced by the average value of these variables. Also, in addition to the anticipated amount or average value, the probability of state variables to be high or low from a given value must be considered:

$$P^{\text{Transmision}} + \sum_{i=1}^{N_{\text{bus}}} {P_i}^{\text{CHP}} + \sum_{i=1}^{N_{\text{bus}}} {P_i}^{\text{Wind}} + \sum_{i=1}^{N_{\text{bus}}} {P_i}^{\text{Battery}} = \sum_{i=1}^{N_{\text{bus}}} {P_i}^{\text{Load}} + P^{\text{Loss}}, \tag{16}$$

$$Q^{\text{Transmision}} + \sum_{i=1}^{N_{\text{bus}}} {Q_i}^{\text{CHP}} + \sum_{i=1}^{N_{\text{bus}}} {Q_i}^{\text{Wind}} = \sum_{i=1}^{N_{\text{bus}}} {Q_i}^{\text{Load}} + Q^{\text{Loss}}. \tag{17}$$

In these two equations, $P^{\text{transmision}}$ and $Q^{\text{transmision}}$ are the active and reactive power taken from the upstream transmission grid, N_{bus} is the number of nodes, ${P_i}^{\text{CHP}}$ and ${Q_i}^{\text{CHP}}$ are the active and reactive power of the ith CHP generator if available, ${P_i}^{\text{Wind}}$ and ${Q_i}^{\text{Wind}}$ are the active and reactive power of the ith wind generator if available, ${Q_i}^{Capacitor}$ is the reactive power generated by the reactive power source of the ith node if available, ${P_i}^{\text{Battery}}$ is the amount of active power generated (or consumed) by the energy storage system of the ith node if available, ${P_i}^{\text{Load}}$ and ${Q_i}^{\text{Load}}$ are the active and reactive power of the load in the ith node, and P^{Loss} and Q^{Loss} are active and reactive power losses of the entire grid.

$$0 \le {P_i}^{\text{CHP}} \le {P_i}^{\overset{\max}{\text{CHP}}}, \tag{18}$$

where ${P_i}^{\overset{\max}{\text{CHP}}}$ is the maximum producible active power by the CHP located at the ith node.

$$-{P_i}^{\overset{\max}{\text{Battery}}} \le {P_i}^{\text{Battery}} \le {P_i}^{\overset{\max}{\text{Battery}}}, \tag{19}$$

where ${P_i}^{\overset{\max}{\text{Battery}}}$ and $-{P_i}^{\overset{\max}{\text{Battery}}}$ are the maximum recharge ability and discharge ability of active power by the energy storage system located in the ith node.

$$0 \le {Q_i}^{\text{Capacitor}} \le {Q_i}^{\overset{\max}{\text{Capacitor}}}, \tag{20}$$

where $Q_i^{\overset{\max}{\text{Capacitor}}}$ is the maximum producible reactive power by the capacitor located at the ith node.

$$0.95 \leq \mathrm{E}\left[V_i\right] \leq 1.05, \tag{21}$$

where V_i is the voltage of the ith node and $\mathrm{E}\left[\right]$ is the operator of the expected or average value.

$$\mathrm{E}\left[I_l\right] \leq \overset{\max}{I_l}, \tag{22}$$

where I_l is the current amount of the lth branch and $\overset{\max}{I_l}$ is the maximum allowable current of the lth line.

$$\mathrm{p}\left(V_i \geq 1.05\right) \leq 0.05, \tag{23}$$

$$\mathrm{p}\left(V_i \leq 0.95\right) \leq 0.05, \tag{24}$$

$$\mathrm{p}\left(I_l \geq \overset{\max}{I_l}\right) \leq 0.05. \tag{25}$$

In (23) to (25), $\mathrm{p}\left(\right)$ is the probability operator of the specified conditions.

5. Problem solving method (particle swarm optimization algorithm)

Various techniques have been introduced for optimization problems to date. Analytical methods that are traditionally based on derivations are robust and effective. However, they encounter some complications such as getting trapped in local minima, increasing computational complexity, and not being applicable to certain classes of objective functions. Heuristic optimization techniques can overcome most of the mentioned difficulties. They are derivative-free, less sensitive to the convexity or continuity nature of the objective functions, able to escape from local minima, and not requiring a good initial solution for starting [40].

Particle swarm optimization (PSO) is a population-based evolutionary optimization technique introduced by Kennedy and Eberhart in 1995. It is easy to implement with few parameters to adjust. Compared with other heuristic methods such as the genetic algorithm (GA), PSO has better computational efficiency and more stable convergence characteristics [41].

In this algorithm, the global optimal solution is obtained using a population of particles. Each particle represents a possible solution of the problem. The algorithm begins with N particles. Each particle in the search space has a current position x_i and a velocity vector v_i. The fitness function of each individual is specified by $F\left(x\right)$. The best individual experience of each particle $x_i^{\text{Localbest}}$ corresponds to the best fitness function of that particle during repetitions. The best collective experience $x^{\text{Globalbest}}$ corresponds to the best individual experience of all particles during repetitions. The steps of this algorithm are as follows:

1. Formation of initial population and initial velocity vectors randomly.
2. Calculating fitness function value of particles according to the current position of each particle.
3. Getting the best individual experience of each particle, $x_i^{\text{Localbest}}$.
4. Getting the best collective experience $x^{\text{Globalbest}}$.

5. Updating the position of particles and velocity vectors based on the best individual and collective experiences in accordance with (26) and (27).

6. Repeating Step 2 until achieving the convergence condition [42].

$$x_i{}^{n+1} = x_i{}^{n} + v_i{}^{n+1}, \tag{26}$$

$$v_i{}^{n+1} = v_i{}^{n} + \rho_1 \times r_1 \times \left(x_i{}^{\text{Localbest}} - x_i{}^{n}\right) + \rho_2 \times r_2 \times \left(x^{\text{Globalbest}} - x_i{}^{n}\right), \tag{27}$$

where $x_i{}^{n}$ and $x_i{}^{n+1}$ are the ith individual or particle in the nth and $n+1$th generations, respectively. $v_i{}^{n}$ and $v_i{}^{n+1}$ are the velocity corresponding to the ith particle in the nth and $n+1$th generation, respectively. ρ_1 and ρ_2 are learning factors of the PSO algorithm. r_1 and r_2 are independent uniform random numbers. $x_i{}^{\text{Localbest}}$ is the best individual experience of the ith particle and $x^{\text{Globalbest}}$ is the best collective experience of particles.

Figure 3 shows the flowchart of problem-solving by PSO method.

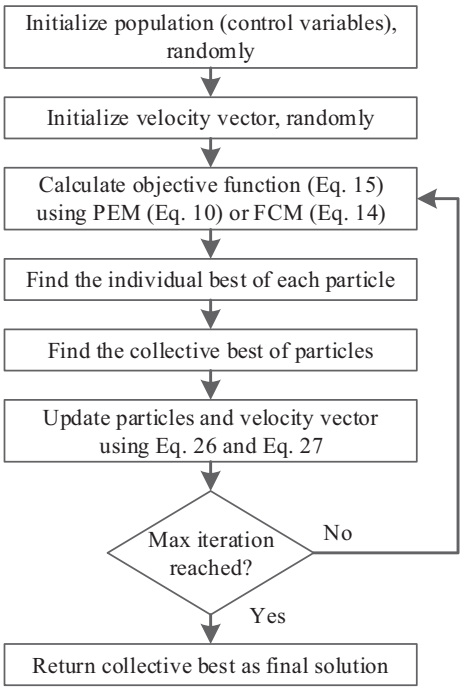

Figure 3. Flowchart of problem-solving by PSO method.

As seen in this figure, objective function calculation needs probabilistic assessment of the distribution system, which can be conducted via (10) or (14).

6. Simulation results and discussions

The IEEE 37-node standard test system is a real distribution system in California. In this system, nominal voltage of the grid is 4.8 kV and the loads are connected in delta Δ configuration. Also, all loads are concentrated and combine active and reactive loads with constant power and the grid is completely unbalanced [43].

A one-line diagram of this system is presented in Figure 4.[1] The values of base active and reactive loads are presented in Table 1. Also, the assumed locations of CHP generators, wind turbines, energy storage systems, and reactive power compensators are shown in this figure. These components' locations are assumed to be distributed all over the grid.

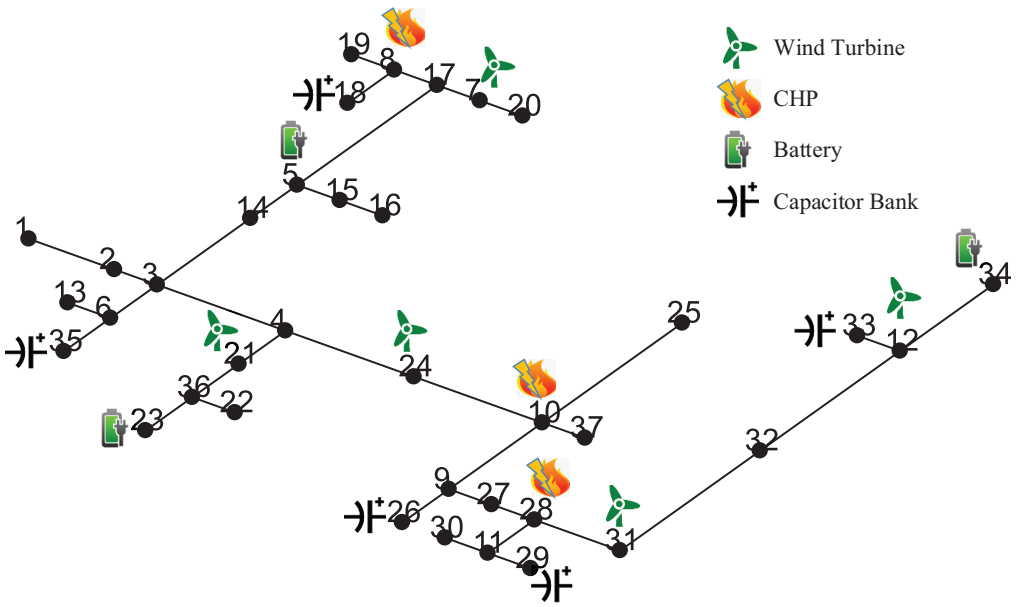

Figure 4. One-line diagram of IEEE 37-node standard test system.

Figure 5 shows the load curve for the studied grid without considering the uncertainty of loads in a 6-h time interval based on the coefficient of the base load amount. In this figure, the amount of grid load in each node, in each phase, and in each hour is obtained by multiplying the k_t coefficient by the base load amount as in (28) and (29):

$$P_{t,i}{}^{\text{Load}} = k_t \times P_{0,i}{}^{\text{Load}}, \tag{28}$$

$$Q_{t,i}{}^{\text{Load}} = k_t \times Q_{0,i}{}^{\text{Load}}, \tag{29}$$

where $i = 1, 2, ..., T$, the superscript 0 refers to the base case, t is the time interval index, and i is the node index. The k_t coefficient is obtained from Figure 5, as said.

Also, it is assumed that the loads on nodes 13, 14, 15, 16, 19, 20, 22, 27, 32, and 37 are random variables that follow normal distribution [34]. It is supposed that the expected values of these variables in various time intervals are equal to their values obtained from (28) and (29). The value of the standard deviation of each load in each time interval is equal to its related expected value divided to 5.

Table 2 shows the probabilistic information related to the wind generators connected to different nodes. The probabilistic distribution of these generators is considered similar to the probability distribution of wind speed. Since the Weibull probability distribution is usually considered for wind speed, this probability distribution is also considered in the generators' output [34].

[1] http://sites.ieee.org/pes-testfeeders/resources/.

Table 1. The value of base active and reactive loads.

Node	Phase a		Phase b		Phase c	
	Active (kW)	Reactive (kVAr)	Active (kW)	Reactive (kVAr)	Active (kW)	Reactive (kVAr)
1	0	0	0	0	0	0
2	140	70	140	70	350	175
3	0	0	0	0	0	0
4	0	0	0	0	0	0
5	0	0	0	0	0	0
6	0	0	0	0	0	0
7	0	0	0	0	0	0
8	0	0	0	0	0	0
9	0	0	0	0	0	0
10	0	0	0	0	0	0
11	0	0	0	0	0	0
12	0	0	0	0	0	0
13	0	0	0	0	85	40
14	0	0	0	0	85	40
15	17	8	21	10	0	0
16	85	40	0	0	0	0
17	0	0	0	0	85	40
18	0	0	140	70	21	10
19	0	0	42	21	0	0
20	0	0	42	21	0	0
21	0	0	0	0	42	21
22	42	21	42	21	42	21
23	42	21	0	0	0	0
24	0	0	0	0	85	40
25	0	0	85	40	0	0
26	0	0	0	0	42	21
27	85	40	0	0	0	0
28	0	0	0	0	42	21
29	0	0	0	0	85	40
30	0	0	42	21	0	0
31	140	70	0	0	0	0
32	126	62	0	0	0	0
33	0	0	0	0	85	40
34	0	0	0	0	42	21
35	8	4	85	40	0	0
36	42	21	0	0	0	0
37	0	0	0	0	0	0

The assumptions related to the CHP power plants are described in Table 3. In addition, assumptions related to energy storage resources are described in Table 4. The assumptions related to the reactive power compensators are described in Table 5.

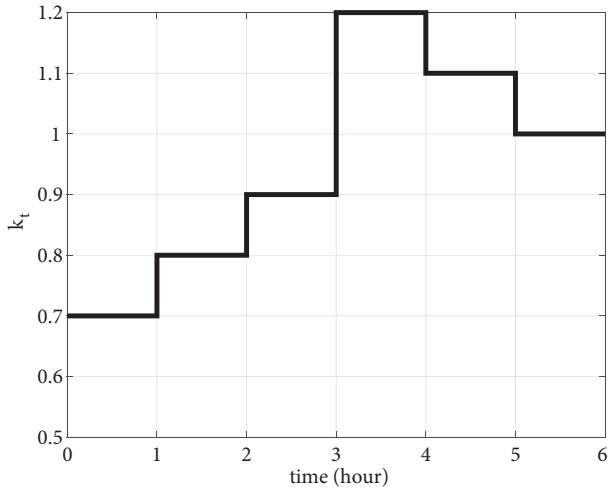

Figure 5. The coefficients of the load curve of the studied grid based on the base load.

Table 2. The probabilistic information of the wind generators connected to different nodes of the studied network.

Node	Scale parameter	Shape parameter	Mean	Standard deviation
7	15	1.8	13.34	7.67
12	15	1.8	13.34	7.67
21	15	1.8	13.34	7.67
24	15	1.8	13.34	7.67
31	15	1.8	13.34	7.67

Table 3. Location and capacity of CHP power plants.

Nodes	Maximum producible power (kW)
8	25
10	25
28	25

Table 4. Location and capacity of energy storage resources available in the studied grid.

Nodes	Maximum chargeability and dischargeability in an hour (kW).
5	15
23	15
34	15

As regards the cost coefficients in the objective function, it is assumed that the cost of power generation in the CHP is equal to the cost of purchasing power from the upstream grid in the base load mode (the sixth time interval of the studied period). The cost of purchasing power from the upstream grid in the first, second, and third time intervals has 10% reduction compared to the base amount. Also, in the fourth and fifth time intervals, there is 10% increase in comparison to base load mode.

Table 5. Location and capacity of reactive power compensators.

Nodes	Number and capacity (kVAr)
18	2 × 25
26	2 × 25
29	2 × 25
33	2 × 25
35	2 × 25

Regarding the PSO algorithm, the number of particles in the swarm is set to 100, the number of total iterations is set to 750, and both of the learning factors ($\rho_1$andρ_2) are set to 2, as usual [42]. It is noticeable that a great number of algorithm iterations can guarantee the convergence and optimality of the solutions.

Regarding probabilistic assessment methods, the number of points in PEM is 2 and the number of clusters in FCM is 10.

In addition, this study is implemented on MATLAB software and the calculation is conducted on an Intel core i7-6500U 2.5 GHz with 8 GB RAM system.

6.1. First scenario

In this scenario, it is assumed that the control variables, except for energy storage sources, have a constant value and do not change over the entire period of the study. However, this type of operating can lead to getting away from the global optimal operating point, but this scenario presents some benefits. The operating point does not need to change and is kept constant during the whole operating interval, and this means that there is no need to run the optimization program in different hours. Also, there are few control variables and less computational complexity is required as a result.

Table 6 and Table 7 show the proposed control variables by the proposed method using PEM and FCM, respectively.

Table 6. Obtained results from applying the proposed algorithm (first scenario) using PEM.

Control variable	Node	Time period					
		first	second	third	fourth	fifth	sixth
Energy storage systems (kW)	5	-15.00	-15.00	-15.00	+15.00	+15.00	+15.00
	23	-15.00	-15.00	-15.00	+15.00	+15.00	+15.00
	34	-15.00	-15.00	-15.00	+15.00	+15.00	+15.00
CHP generators (kW)	8	2.13					
	10	22.76					
	28	0.46					
Reactive power compensators (kVAr)	18	50.00					
	26	50.00					
	29	50.00					
	33	25.00					
	35	25.00					

Table 7. Obtained results from applying the proposed algorithm (first scenario) using FCM.

Control variable	Node	Time period					
		first	second	third	fourth	fifth	sixth
Energy storage systems (kW)	5	-15.00	-15.00	-15.00	+15.00	+15.00	+15.00
	23	-15.00	-15.00	-15.00	+15.00	+15.00	+15.00
	34	-15.00	-15.00	-15.00	+15.00	+15.00	+15.00
CHP generators (kW)	8	4.41					
	10	19.12					
	28	1.76					
Reactive power compensators (kVAr)	18	50.00					
	26	50.00					
	29	50.00					
	33	25.00					
	35	25.00					

The results of Table 6 and Table 7 can be discussed as follows. As seen, the results of the two methods are very close to each other and this shows the relative convergence of the optimization algorithm. All energy storage systems are fully charged at low load hours (with less cost) like the first, second, and third hours and are discharged at peak load hours (with higher cost) like the fourth, fifth, and sixth hours. This can be attributed to the cost ignorance for charge and discharge of these systems.

Considering the fact that the cost of CHP generators is approximately equal to the cost of purchasing power from the upstream grid, it is expected that there will be a greater tendency to use the full capacity of these generators. However, according to Table 6 and Table 7, the full capacity of these generators is not used. If the total capacities of these generators are used at low load hours, more cost will be imposed to the grid operator. However, the grid operator has a tendency to buy power from the upstream grid during low load hours due to the low energy prices at these hours.

In addition, in the proposed solution, the maximum values for reactive power compensators have not been allocated. In most nodes the load amount is zero and dedicating the possible maximum values for reactive power compensator resources will exceed the voltage range beyond the upper limit.

6.2. Second scenario

In this scenario it is assumed that all control variables can be varied during all the study time periods like energy storage systems. This scenario presents some benefits. The operating program in this scenario is completely flexible and it is possible to reach the global optimum operating points. Also, there are some drawbacks and difficulties in this scenario. The optimization program must be run every different hour. A large number of control variables are involved and computational complexity is increased consequently. The operating point needs to change continuously over the whole time interval.

Table 8 and Table 9 show the obtained results of applying the proposed algorithm using PEM and FCM, respectively.

The results of Table 8 and Table 9 can be described as follows. As seen, the results of the two methods are very close to each other and this shows the relative convergence of the optimization algorithm. All energy

Table 8. Obtained results from applying the proposed algorithm (second scenario) using PEM.

Control variable	Node	Time period					
		first	second	third	fourth	fifth	sixth
Energy storage resources (KW)	5	-15.00	-15.00	-15.00	+15.00	+15.00	+15.00
	23	-15.00	-15.00	-15.00	+15.00	+15.00	+15.00
	34	-15.00	-15.00	-15.00	+15.00	+15.00	+15.00
CHP generators (KW)	8	0.00	0.00	0.00	25.00	25.00	25.00
	10	0.00	0.00	0.00	25.00	25.00	25.00
	28	0.00	0.00	0.00	25.00	25.00	25.00
Reactive power compensators (KVAr)	18	50.00	50.00	50.00	50.00	50.00	50.00
	26	0.00	50.00	25.00	25.00	50.00	50.00
	29	50.00	25.00	25.00	50.00	0.00	50.00
	33	25.00	50.00	25.00	25.00	50.00	0.00
	35	25.00	50.00	0.00	50.00	0.00	50.00

Table 9. Obtained results from applying the proposed algorithm (second scenario) using FCM.

Control variable	Node	Time period					
		first	second	third	fourth	fifth	sixth
Energy storage resources (KW)	5	-15.00	-15.00	-15.00	+15.00	+15.00	+15.00
	23	-15.00	-15.00	-15.00	+15.00	+15.00	+15.00
	34	-15.00	-15.00	-15.00	+15.00	+15.00	+15.00
CHP generators (KW)	8	0.00	0.00	0.00	25.00	25.00	25.00
	10	0.00	0.00	0.00	25.00	25.00	25.00
	28	0.00	0.00	0.00	25.00	25.00	25.00
Reactive power compensators (KVAr)	18	50.00	50.00	50.00	50.00	50.00	50.00
	26	25.00	50.00	25.00	50.00	50.00	50.00
	29	50.00	25.00	25.00	50.00	0.00	25.00
	33	25.00	50.00	25.00	25.00	50.00	0.00
	35	50.00	50.00	0.00	50.00	25.00	50.00

storage systems are charged at low load hours like the first, second, and third hours maximally and are discharged during peak load hours like the fourth, fifth, and sixth hours. This is because of the lack of consideration of cost for charging and discharging of these resources.

According to Table 8 and Table 9, the output of CHP generators at low load hours is equal to zero, while at peak load hours, the full capacity of these generators has been used. This is due to the lower price of power purchased from the upstream grid in low load hours than the cost of power generation at CHP generators, and the higher cost of purchased power from the upstream grid in peak load hours compared to the price of power generation at these generators.

Also, at the sixth hour, when the cost of power purchased from the upstream grid is equal to the cost of power generation in CHP generators, since more production of CHP generators leads to a further reduction in losses, there is a tendency to use all the capacity of these generators.

In the proposed solution, the maximum possible amounts for reactive power compensator sources have not been allocated. The reason for this issue is related to the nature of grid loads, since in most nodes the load amount is zero and assigning the maximum possible values for reactive power compensator sources can cause the voltage range to exceed the upper limit of the voltage amount. Also, some values of reactive power compensator sources are different by the two methods. This is due to this variable discrete nature that can only get three 0, 25, and 50 values.

Various components of the objective function in the two mentioned scenarios by the mentioned methods are compared in Table 10.

Recall that $\sum_{t=1}^{T}\left(\sum_{i=1}^{N_{\mathrm{CHP}}} {P_{t,i}}^{\mathrm{CHP}}\right)$ is the sum of all CHP generators' active power generation in all time intervals, $\sum_{t=1}^{T}\left(\mathrm{E}\left[{P_t}^{\mathrm{Transmision}}\right]\right)$ is the expected active power taken from the upstream grid, and $\sum_{t=1}^{T}\left(w1_t \times \mathrm{E}\left[{P_t}^{\mathrm{Transmision}}\right] + \sum_{i=1}^{N_{\mathrm{CHP}}} w2_{t,i} \times {P_{t,i}}^{\mathrm{CHP}}\right)$ is the objective function as in (15). $\sum_{t=1}^{T}\mathrm{E}\left[{P_t}^{\mathrm{Loss}}\right]$ is the expected value of active power losses in all time intervals.

Table 10. The various component values of the objective function in two scenarios by two methods.

Method	Scenario	$\sum_{t=1}^{T}\left(\sum_{i=1}^{N_{\mathrm{CHP}}} {P_{t,i}}^{\mathrm{CHP}}\right)$	$\sum_{t=1}^{T}\left(\mathrm{E}\left[{P_t}^{\mathrm{Transmision}}\right]\right)$	$\sum_{t=1}^{T}\left(w1_t \times \mathrm{E}\left[{P_t}^{\mathrm{Transmision}}\right]\right) + \sum_{t=1}^{T}\left(\sum_{i=1}^{N_{\mathrm{CHP}}} w2_{t,i} \times {P_{t,i}}^{\mathrm{CHP}}\right)$	$\sum_{t=1}^{T}\mathrm{E}\left[{P_t}^{\mathrm{Loss}}\right]$
PEM	First	456.2370 (kW)	1.2716 e+04 (kW)	1.3108 e+04	122.3806 (kW)
	Second	675 (kW)	1.2491 e+04 (kW)	1.3048 e+04	116.1499 (kW)
FCM	First	455.2200 (kW)	1.2653 e+04 (kW)	1.3105 e+04	122.3277 (kW)
	Second	675 (kW)	1.2490 e+04 (kW)	1.3047 e+04	115.7852 (kW)

According to the values given in Table 6, Table 7, and Table 10, the total power generation at the CHP generators in the first scenario is equal to 456.23 MW, which is lower compared to the maximum capacity of total generation during all the studied periods, i.e. 1350 MW. The reason for this is the low price of energy at low load hours and the tendency of the operator to buy the power from the upstream grid.

Moreover, based on Table 8, Table 9, and Table 10, the total power generation amount at CHP generators in the second scenario is equal to 675 MW, which is lower compared to the total capacity of generation during the whole studied periods, i.e. 1350 MW. The reason for this is the low price of energy at low load hours and the tendency of the operator to buy the power from the upstream grid, as mentioned earlier.

From Table 10, the following cases can be deduced.

The expected cost in the first scenario is higher than the expected cost in the second scenario. In fact, this higher cost is due to the constant production of CHP generators in the first scenario, which has less flexibility than the second scenario.

Also, the expected value of the power purchased from the upstream grid in the first scenario is higher than this value in the second scenario. This is due to the higher total amount of power generation at the CHP generators in the second scenario compared to the first scenario. This issue causes the expected amount of losses in the second scenario to be lower than in the first scenario, because in the second scenario, more CHP generators are used.

Probabilistic information of the distribution system can be obtained from these studies. Table 11 shows the probabilistic information of the amount of power obtained from the upstream transmission grid during the studied time in two scenarios by PEM. The information of this table helps the operator to make risk-based decisions.

Table 11. Probabilistic information of the amount of power obtained from the upstream transmission grid by PEM.

Hour	First scenario		Second scenario	
	Mean	Standard deviation	Mean	Standard deviation
First	1620.2504	62.1591	1697.3197	62.2314
Second	1874.0747	64.9832	1951.2431	65.0030
Third	2128.5693	68.0498	2206.3522	68.1386
Fourth	2619.9443	78.2253	2466.9092	78.0596
Fifth	2364.0088	74.5873	2211.9059	74.4430
Sixth	2108.7592	71.1215	1956.8827	70.9757

Table 12 compares the performance of the PEM and FCM in the proposed method. As seen, the run time of FCM is meaningfully less than PEM and it is more appropriate for online applications.

Table 12. Comparing the performance of PEM and FCM in the proposed method.

Method	Scenario	Calculation time (seconds)
PEM	First	223.2
	Second	280.8
FCM	First	30.4
	Second	43.1

7. Conclusion

In this paper, robust operation of smart distribution grids was considered. The studied distribution system is an unbalanced system including wind generators with probabilistic output and also probabilistic loads that was equipped with energy storage systems, CHP generators, and a reactive power compensator. As the situation of the distribution system may vary in a wide range, the robustness of the operating point is very important. In these studies, computational complexity of probabilistic assessment methods is remarkable besides their ability in presenting accurate results.

An optimal operating program that can satisfy all possible conditions was considered in two scenarios. In the first scenario, the operating variables were considered constant during the study period, and in the second scenario, the control variables had the ability to vary during the operating time. The advantages and disadvantages of the operating instructions were discussed. Keeping the control variables constant during the study time (the first scenario) makes it less flexible than the state in which the control variables can change during the study time (second scenario). This would increase the expected cost of operation in the first scenario in spite of the simplicity of the operating instructions. In the first scenario, due to the constant amount of control variables during the entire operating time, the amount of control variables has been affected by the entire duration of the study, not just a specific hour. In the second scenario, due to greater flexibility, the objective

function has been reduced to a greater extent. However, the second scenario encounters some problems such as greater computational complexity, difficulties in implementing operating instructions, probability of failing to implement these instructions, and so on.

In addition, the applications of two probabilistic assessment methods, i.e. the point estimation method and fuzzy clustering method, were considered and compared in terms of calculation complexity and calculation burden time aspects in this study.

Finally, the risk factors for buying power from upstream have been calculated in this paper, which can be very important for the grid operator in terms of validity and certainty of decision-making.

References

[1] Galvani S, Choogan M. Data clustering based probabilistic optimal power flow in power systems. IET Generation, Transmission & Distribution 2018; 13 (2): 181-188. doi: 10.1049/iet-gtd.2018.5832

[2] Rahbar K, Xu J, Zhang R. Real-time energy storage management for renewable integration in microgrid: An off-line optimization approach. IEEE Transactions on Smart Grid 2015; 6 (1): 124-134. doi: 10.1109/TSG.2014.2359004

[3] Yang Z, Wu R, Yang J, Long K, You P. Economical operation of microgrid with various devices via distributed optimization. IEEE Transactions on Smart Grid 2016; 7 (2): 857-867. doi: 10.1109/TSG.2015.2479260

[4] Battistelli C, Agalgoankar YP, Pal BC. Probabilistic dispatch of remote hybrid microgrids including battery storage and load management. IEEE Transactions on Smart Grid 2017; 8 (3): 1305-1317. doi: 10.1109/TSG.2016.2606560

[5] Nikmehr N, Najafi-Ravadanegh S. Optimal operation of distributed generations in micro-grids under uncertainties in load and renewable power generation using heuristic algorithm. IET Renewable Power Generation 2015; 9 (8): 982-990. doi: 10.1049/iet-rpg.2014.0357

[6] Wang Z, Chen B, Wang J, Kim J, Begovic MM. Robust optimization based optimal DG placement in microgrids. IEEE Transactions on Smart Grid 2014; 5 (5): 2173-2182. doi: 10.1109/TSG.2014.2321748

[7] Zare M, Niknam T, Azizipanah-Abarghooee R, Ostadi A. New stochastic bi-objective optimal cost and chance of operation management approach for smart microgrid. IEEE Transactions on Industrial Informatics 2016; 12 (6): 2031-2040. doi: 10.1109/TII.2016.2585379

[8] Bahmani-Firouzi B, Azizipanah-Abarghooee R. Optimal sizing of battery energy storage for micro-grid operation management using a new improved bat algorithm. International Journal of Electrical Power & Energy Systems 2014; 56: 42-54. doi: 10.1016/j.ijepes.2013.10.019

[9] Carpinelli G, Mottola F, Proto D. Probabilistic sizing of battery energy storage when time-of-use pricing is applied. Electric Power Systems Research 2016; 141: 73-83. doi: 10.1016/j.epsr.2016.07.013

[10] Chakraborty S, Okabe T. Robust energy storage scheduling for imbalance reduction of strategically formed energy balancing groups. Energy 2016; 114: 405-417. doi: 10.1016/j.energy.2016.07.170

[11] Craparo E, Karatas M, Singham DI. A robust optimization approach to hybrid microgrid operation using ensemble weather forecasts. Applied Energy 2017; 201: 135-147. doi: 10.1016/j.apenergy.2017.05.068

[12] Kou P, Gao F, Guan X. Stochastic predictive control of battery energy storage for wind farm dispatching: Using probabilistic wind power forecasts. Renewable Energy 2015; 80: 286-300. doi: 10.1016/j.renene.2015.02.001

[13] Soroudi A. Robust optimization based self scheduling of hydro-thermal Genco in smart grids. Energy 2013; 61: 262-271. doi: 10.1016/j.energy.2013.09.014

[14] Li P, Xu D, Zhou Z, Lee WJ, Zhao B. Stochastic optimal operation of microgrid based on chaotic binary particle swarm optimization. IEEE Transactions on Smart Grid 2016; 7 (1): 66-73. doi: 10.1109/TSG.2015.2431072

[15] Guggilam SS, Dall'Anese E, Chen YC, Dhople SV, Giannakis GB. Scalable optimization methods for distribution networks with high PV integration. IEEE Transactions on Smart Grid 2016; 7 (4): 2061-2070. doi: 10.1109/TSG.2016.2543264

[16] Ziadi Z, Taira S, Oshiro M, Funabashi T. Optimal power scheduling for smart grids considering controllable loads and high penetration of photovoltaic generation. IEEE Transactions on Smart Grid 2014; 5 (5): 2350-2359. doi: 10.1109/TSG.2014.2323969

[17] Arefifar SA, Ordonez M, Mohamed YA. VI controllability-based optimal allocation of resources in smart distribution systems. IEEE Transactions on Smart Grid 2016; 7 (3): 1378-1388. doi: 10.1109/TSG.2015.2476784

[18] Awad AS, El-Fouly TH, Salama MM. Optimal ESS allocation for load management application. IEEE Transactions on Power Systems 2015; 30 (1): 327-336. doi: 10.1109/TPWRS.2014.2326044

[19] Awad AS, El-Fouly TH, Salama MM. Optimal ESS allocation and load shedding for improving distribution system reliability. IEEE Transactions on Smart Grid 2014; 5 (5): 2339-2349. doi: 10.1109/TSG.2014.2316197

[20] Awad AS, El-Fouly TH, Salama MM. Optimal ESS allocation for benefit maximization in distribution networks. IEEE Transactions on Smart Grid 2017; 8 (4): 1668-1678. doi: 10.1109/TSG.2015.2499264

[21] Luh PB, Yu Y, Zhang B, Litvinov E, Zheng T et al. Grid integration of intermittent wind generation: a Markovian approach. IEEE Transactions on Smart Grid 2014; 5 (2): 732-741. doi: 10.1109/TSG.2013.2268462

[22] Zou K, Agalgaonkar AP, Muttaqi KM, Perera S. An analytical approach for reliability evaluation of distribution systems containing dispatchable and nondispatchable renewable DG units. IEEE Transactions on Smart Grid 2014; 5 (6): 2657-2665. doi: 10.1109/TSG.2014.2350505

[23] Abdeltawab HH, Mohamed YA. Robust operating zones identification for energy storage day-ahead operation. Sustainable Energy, Grids and Networks 2017; 10: 1-11. doi: 10.1016/j.segan.2017.02.002

[24] Liu S, Liu F, Ding T, Bie Z. Optimal allocation of reactive power compensators and energy storages in microgrids considering uncertainty of photovoltaics. Energy Procedia 2016; 103: 165-170. doi: 10.1016/j.egypro.2016.11.267

[25] Xiang Y, Liu J, Liu Y. Robust energy management of microgrid with uncertain renewable generation and load. IEEE Transactions on Smart Grid 2016; 7 (2): 1034-1043. doi: 10.1109/TSG.2014.2385801

[26] Simão HP, Jeong HB, Defourny B, Powell WB, Boulanger A et al. A robust solution to the load curtailment problem. IEEE Transactions on Smart Grid 2013; 4 (4): 2209-2219. doi: 10.1109/TSG.2013.2276754

[27] Mostafa HA, El Shatshat R, Salama MM. Optimal distribution systems operation using smart matching scheme (SMS) for smart grid applications. IEEE Transactions on Smart Grid 2014; 5 (4): 1938-1948. doi: 10.1109/TSG.2013.2294055

[28] Vallée F, Brunieau G, Pirlot M, Deblecker O, Lobry J. Optimal wind clustering methodology for adequacy evaluation in system generation studies using nonsequential Monte Carlo simulation. IEEE Transactions on Power Systems 2011; 26 (4): 2173–2184. doi: 10.1109/TPWRS.2011.2138726

[29] Gang L, Jinfu C, Defu C, Dongyuan S, Xianzhong D. Probabilistic assessment of available transfer capability considering spatial correlation in wind power integrated system. IET Generation, Transmission & Distribution 2013; 7 (12): 1527–1535. doi: 10.1049/iet-gtd.2013.0081

[30] Hagh MT, Amiyan P, Galvani S, Valizadeh N. Probabilistic load flow using the particle swarm optimisation clustering method. IET Generation, Transmission & Distribution 2017; 12 (3): 780–789. doi: 10.1049/iet-gtd.2017.0678

[31] Hasanvand S, Nayeripour M, Arefifar SA, Fallahzadeh-Abarghouei H. Spectral clustering for designing robust and reliable multi-MG smart distribution systems. IET Generation, Transmission & Distribution 2017; 12 (6): 1359–1365. doi: 10.1049/iet-gtd.2017.0671

[32] Lami B, Bhattacharya K. Clustering technique applied to nodal reliability indices for optimal planning of energy resources. IEEE Transactions on Power Systems 2016; 31 (6): 4679–4690. doi: 10.1109/TPWRS.2015.2507061

[33] Munshi AA, Yasser ARM. Photovoltaic power pattern clustering based on conventional and swarm clustering methods. Solar Energy 2016; 124: 39–56. doi: 10.1016/j.solener.2015.11.010

[34] Galloway SJ, Elders IM, Burt GM, Sookananta B. Optimal flexible alternative current transmission system device allocation under system fluctuations due to demand and renewable generation. IET Generation, Transmission & Distribution 2010; 4 (6): 725-735. doi: 10.1049/iet-gtd.2009.0221

[35] Mohammadi M. Probabilistic harmonic load flow using fast point estimate method. IET Generation, Transmission & Distribution 2015; 9 (13): 1790-1799. doi: 10.1049/iet-gtd.2014.0669

[36] Morales JM, Perez-Ruiz J. Point estimate schemes to solve the probabilistic power flow. IEEE Transactions on Power Systems 2007; 22 (4): 1594-1601. doi: 10.1109/TPWRS.2007.907515

[37] Liu Y, Sioshansi R, Conejo AJ. Hierarchical clustering to find representative operating periods for capacity-expansion modeling. IEEE Transactions on Power Systems 2017; 33 (3): 3029–3039. doi: 10.1109/TPWRS.2017.2746379

[38] Dunn JC. A fuzzy relative of the ISODATA process and its use in detecting compact well-separated clusters. Journal of Cybernetics 1973; 3 (3): 32-57. doi: 10.1080/01969727308546046

[39] Lai CS, Jia Y, McCulloch MD, Xu Z. Daily clearness index profiles cluster analysis for photovoltaic system. IEEE Transactions on Industrial Informatics 2017; 13 (5): 2322–2332. doi: 10.1109/TII.2017.2683519

[40] AlRashidi MR, El-Hawary ME. A survey of particle swarm optimization applications in electric power systems. IEEE Transactions on Evolutionary Computation 2009; 13 (4): 913-918. doi: 10.1109/TEVC.2006.880326

[41] Su X, Masoum MA, Wolfs PJ. PSO and improved BSFS based sequential comprehensive placement and real-time multi-objective control of delta-connected switched capacitors in unbalanced radial MV distribution networks. IEEE Transactions on Power Systems 2016; 31 (1): 612-622. doi: 10.1109/TPWRS.2015.2398361

[42] Haupt RL, Haupt SE. Practical Genetic Algorithms. 2nd ed. New York, NY, USA: Wiley, 2004.

[43] Kersting WH. Radial distribution test feeders. In: IEEE 2001 Power Engineering Society Winter Meeting; 2001. pp. 908-912.